

SHORT
COMMUNICATIONS

Formation of Spherical Voids in the Oxidation of Co Nanoparticles

P. A. Chernavskii^a, G. V. Pankina^a, V. I. Zaikovskii^b, N. V. Peskov^c, and V. V. Lunin^a

^a Faculty of Chemistry, Moscow State University, Leninskie gory, Moscow, 119992 Russia

^b Boreskov Institute of Catalysis, Siberian Branch, Russian Academy of Sciences,
pr. Akademika Lavrent'eva 5, Novosibirsk, 630090 Russia

^c Faculty of Computational Mathematics and Cybernetics, Moscow State University, Leninskie gory, Moscow, 119992 Russia

e-mail: chern@kge.chem.msu.ru

Received April 23, 2007

Abstract—A high-resolution transmission microscopy study showed that the oxidation of Co nanoparticles deposited on montmorillonite resulted in the formation of nanoshells consisting of cobalt oxides and containing spherical voids. A linear dependence was found between the initial diameter of Co particles and the oxide shell thickness.

DOI: 10.1134/S0036024408040341

INTRODUCTION

As is known, high-temperature oxidation of metals during the formation of thick oxide layers at the metal–oxide interface causes the formation of voids as a result of the association of vacancies, which appear because of the difference between the diffusion coefficients of metal ions and oxygen [1–3].

Recently, a similar phenomenon was observed in the oxidation of Co [4] and Fe [5] nanoparticles at relatively low temperatures. High-resolution electron microscopy showed that the low-temperature oxidation of Co and Fe nanoparticles led to the accumulation of vacancies at the metal–oxide interface and formation of spherical voids within metal oxide shells.

This phenomenon has the following explanation. Oxide films grow either at the metal–oxide interface (oxygen ion transport inside particles) or at the oxide–gas boundary (metal ion transport to the surface), which depends on the type of migrating lattice defects. When the difference in the diffusion coefficients is large (Kirkendall effect), regions with vacancies are formed at the metal–oxide interface, and the accumulation of vacancies leads to the formation of voids.

It was found [5] that, for Fe nanoparticles, there was a critical size (8 nm) at which they were completely oxidized at 20°C, and spherical voids formed inside oxide shells; for large-sized particles, only separate voids, however, formed at the metal–oxide interface. The critical sizes of metal particles at which particle oxidation resulted in the formation of spherical voids was studied theoretically [6]. The thermal instability of spherical nanoshells was considered, and the results of Monte Carlo simulation of the kinetics of nanoshell formation were reported.

EXPERIMENTAL

Co nanoparticles on montmorillonite were prepared by impregnating the support with a solution of cobalt nitrate of kh. ch. (chemically pure) grade. Grade F-160 montmorillonite with a specific surface area of 300 m²/g and the mean pore size 6.6 nm was used as a support. After impregnation, the sample was dried in a flow of air at 100°C for 3 h. As a result, a 20% Co/montmorillonite sample (denoted below as Co/M) was obtained. The dry sample was reduced under hydrogen in a flow microreactor, which was simultaneously the measuring cell of a vibration magnetometer [7]. Reduction was performed in a temperature-programmed mode (TPR) at temperatures of up to 700°C at a heating rate of 0.47 K/s until the degree of reduction ceased to change. The degree of reduction was monitored by measuring changes in magnetization. Magnetization constant in time indicated that the limiting degree of reduction was achieved at the given temperature. The sample was cooled to 200°C in a flow of H₂; H₂ was then replaced with Ar to remove adsorbed hydrogen, and the sample was cooled to room temperature.

Cobalt nanoparticles were subjected to temperature-programmed oxidation (TPO) in a 1% O₂/He flow (heating rate 0.47 K/s). After magnetization decreased to zero, the sample was cooled in an Ar flow to ~20°C and removed from the reactor. It was then examined by high-resolution transmission electron microscopy on a JEM-2010 electron microscope (JEOL, Japan) with a grid resolution of 0.14 nm at an accelerating voltage of 200 kV. The sample was fixed on a standard copper grid.

In addition, the Co/M sample was studied by the TPR method, and changes in magnetization and hydrogen absorption rate were recorded concurrently. This combination of methods allowed us to obtain additional

information about the sequence of stages during reduction [7]. We used a 5% H₂ + Ar mixture instead of H₂.

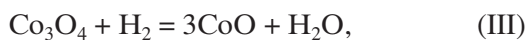
RESULTS AND DISCUSSION

Figures 1 and 2 show the photomicrographs of the 20%Co/M sample after reduction in the TPR mode to 700°C followed by oxidation in the TPO mode to 200°C. The photomicrographs clearly show ring structures, which are nanospherical shells consisting of Co oxide.

The reactions



occur sequentially during the oxidation of Co nanoparticles; reactions



occur during reduction.

To determine exactly what oxide was formed in our experiments, the starting sample obtained after calcining and the sample obtained after the sequence of oxidation and reduction processes were examined by the TPR method using a 5% H₂ + Ar mixture as a reducing agent. Figure 3 shows the temperature dependences of the hydrogen absorption rate and changes in the magnetization of the starting sample, preliminarily calcined under Ar at 400°C for 1 h.

The peak on the hydrogen absorption rate curve in the temperature range 200–300°C is not accompanied by a change in magnetization and corresponds to reaction (III). At 350°C, magnetization increases, which corresponds to the beginning of reaction (IV). The non-monotonic character of hydrogen absorption in this temperature range is possibly caused by mass transfer in support micropores [8]. After the completion of TPR, the sample was oxidized in a 1% O₂ + He flow at a temperature increased linearly from 20 to 250°C and then again subjected to reduction in the TPR mode in 5% H₂ + Ar. The results of repeated reduction are given in Fig. 4.

It follows from the data shown in Fig. 4 that, over the range 200–300°C, we again observe the hydrogen absorption peak corresponding to reaction (III). This shows that the oxidation under the conditions described above produces Co₃O₄. It, however, follows from the ratio of the peak areas in the TPR spectrum that the system contains not only Co₃O₄, but also CoO in both cases. The CoO fraction noticeably increased from 26 to 33% after repeated TPR. We can therefore assume that spherical oxide shells observed in photomicrographs consist mainly of Co₃O₄, but CoO is also present, and the ratio between CoO and Co₃O₄ is approximately 1/3.

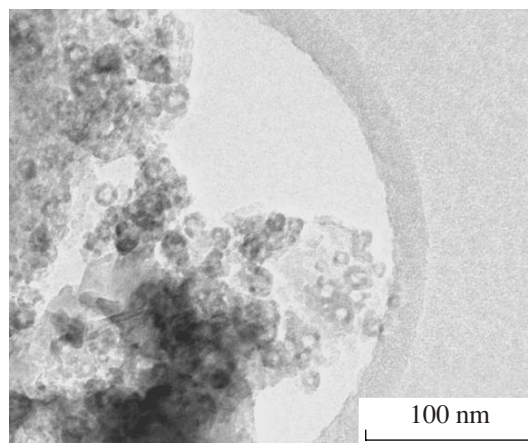


Fig. 1. Electron photomicrograph of the 20% Co/M sample after oxidation in the TPO mode to 200°C.

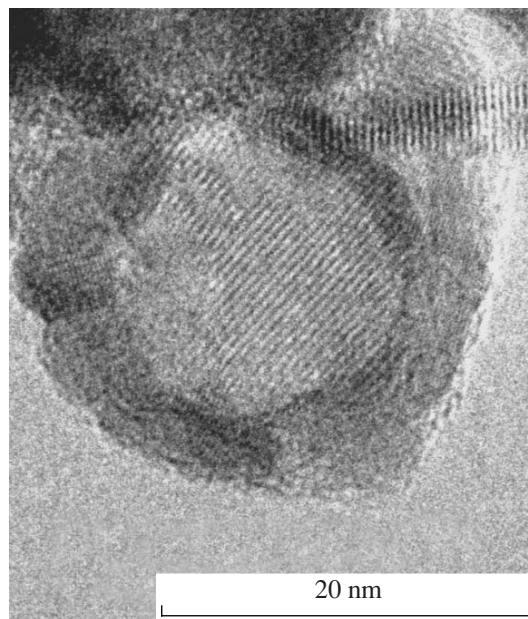


Fig. 2. Photomicrograph of a Co particle on montmorillonite after complete oxidation in the TPO mode in an air flow.

Figure 5 shows the transmission electron microscopy data, namely, the dependence of the thickness δ of nanospherical shells on the inside diameter of voids d .

It follows from the stoichiometry of reactions (I) and (II) that

$$n_{\text{Co}} = n_{\text{CoO}} \quad \text{or} \quad n_{\text{Co}} = (1/3)n_{\text{Co}_3\text{O}_4}, \quad (1)$$

where n_i is the number of moles of Co, CoO, and Co₃O₄ in the starting nanoparticle and spherical oxide shell. The spherical Co particle of diameter d_0 contains n_{Co} moles,

$$n_{\text{Co}} = \frac{\pi \rho_{\text{Co}}}{6M_{\text{Co}}} d_0^3, \quad (2)$$

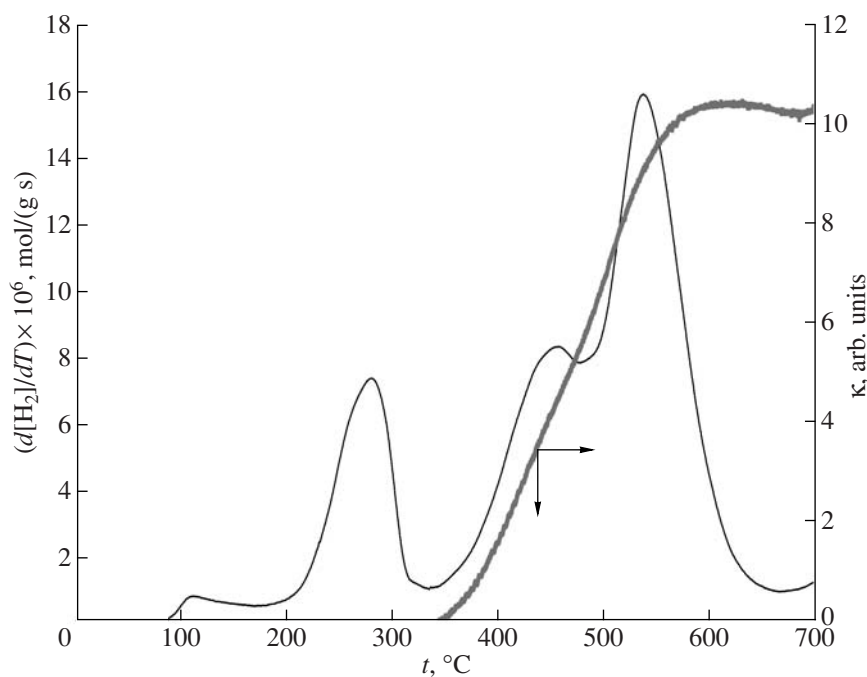


Fig. 3. TPR spectrum and temperature dependence of magnetization (κ) for the starting Co/M sample.

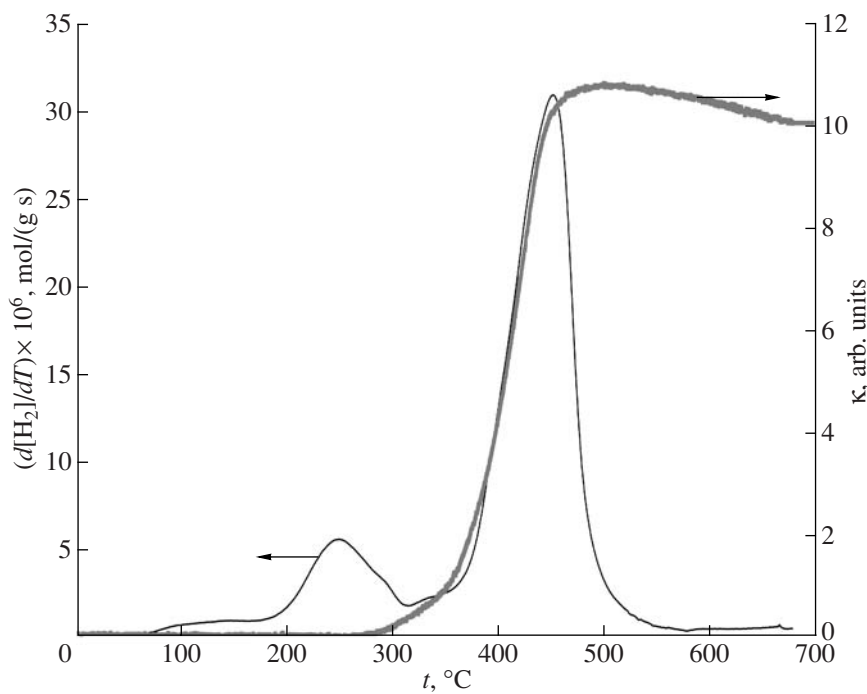


Fig. 4. TPR spectrum and temperature dependence of magnetization for the Co/M sample after the redox process.

where ρ is the density and M is the atomic weight. In a similar way, for Co_3O_4 , we can write

$$n_{\text{Co}_3\text{O}_4} = \frac{\pi \rho_{\text{Co}_3\text{O}_4}}{6M_{\text{Co}_3\text{O}_4}} (D^3 - d^3), \quad (3)$$

where D is the outside diameter of the particle after complete oxidation and d is the diameter of the spherical void formed in place of the Co particle of diameter d_0 .

Suppose the diameter of the spherical void and the diameter of the starting Co particle are related as

$$d = d_0 - \varepsilon,$$

where ε is a parameter. For $\varepsilon = 0$, the oxide film grows only by metal ion diffusion to the oxide–gas interface; in other words, the oxide film grows only at the expense of increasing the oxide film thickness at the gas–oxide interface. For $\varepsilon > 0$, the oxide film grows not only by metal ion diffusion, but also by the counterdiffusion of oxygen ions and the diffusion of vacancies toward the gas–oxide interface.

Taking into account (2) and (3), we can use (1) to derive the dependence of the thickness of the spherical oxide shell on the diameter of a spherical void,

$$\delta = \left[\left(\frac{d + \varepsilon}{2} \right)^3 \frac{1}{C} + \left(\frac{d}{2} \right)^3 \right]^{1/3} - \frac{d}{2}, \quad (4)$$

where $C = V(\text{Co})/V(\text{CoO}) = 0.548$ for the CoO nanoshell and $C = V(\text{Co})/3V(\text{Co}_3\text{O}_4) = 0.056$ for the Co_3O_4 shell. Here, V is the molar volume of Co and oxides. As was shown above, the oxide shell actually contained ~33% CoO and ~67% Co_3O_4 . In addition, it should be taken into account that the density of bulk oxide is obviously different from that of oxide in a nanoshell, and the exact value of C is therefore unknown. The unknown ε and C parameters can be evaluated from the experimental data available using the method of least squares. We obtained $\varepsilon = 2.66$ and $C = 0.35$; the sum of the squares of deviations depended only slightly on the C parameter.

A comparison of the results of the regression analysis and above calculations suggests that the diameter of a spherical void is smaller than that of the starting Co particle. At the first stage of oxidation, several external Co atomic layers are obviously oxidized in situ by oxygen diffusion inside the particle. The Co ions then diffuse under the action of the Mott potential through the oxide layer toward the particle surface and are oxidized there, augmenting the oxide film at the top. Attempts to take into account the mixed composition of the oxide film did not significantly change the estimates of the ε and C parameters in the linear dependence of the oxide layer thickness on the spherical void diameter.

Calculations by (4) showed that zero spherical void diameter, $d = 0$ (the absence of a spherical void inside a particle), corresponded to the particle diameter $d_0 \approx 2$ nm. This value was considered an estimate of a certain critical size of the particle, starting with which the

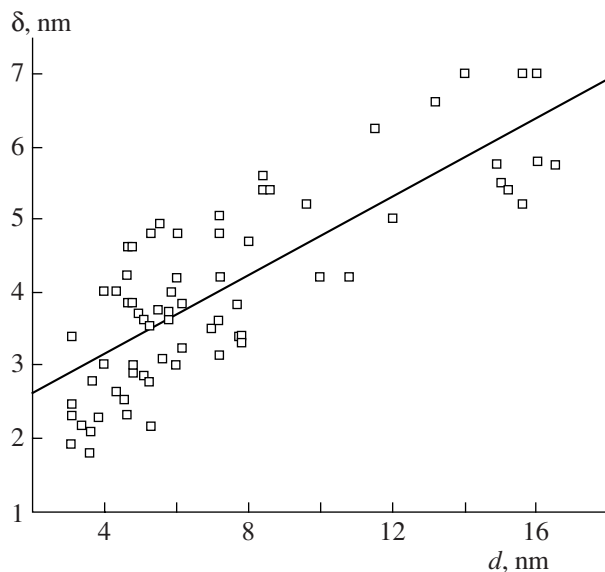


Fig. 5. Dependence of the oxide shell thickness δ on the spherical void diameter d for the Co/M sample. The solid line corresponds to Eq. (4) with the parameters $\varepsilon = 2.66$ and $C = 0.35$.

oxidation is accompanied by the formation of spherical voids.

ACKNOWLEDGMENTS

This work was financially supported by the Russian Foundation for Basic Research (project no. 06-03-32500a) and the Federal Scientific and Technological Program (grant no. 2005-RI-112.0/001/056).

REFERENCES

1. A. Atkinson, *Rev. Mod. Phys.* **57**, 437 (1985).
2. P. Kofstad, *High Temperature Corrosion* (Elsevier Applied Science, London, 1988).
3. T. C. Rojas, J. M. Greneche, A. Conde, and A. Fernandez, *J. Mater. Sci.* **39**, 4877 (2004).
4. Y. Yin, R. M. Riou, C. K. Erdonmez, et al., *Science* (Washington, D.C.) **304**, 711 (2004).
5. C. M. Wang, D. R. Baer, L. E. Thomas, et al., *J. Appl. Phys.* **98**, 094308 (2005).
6. A. M. Gusak, T. V. Zaporozhets, K. N. Tu, and U. Gossele, *Philos. Mag.* **85**, 4445 (2005).
7. P. A. Chernavskii, A. Y. Khodakov, G. V. Pankina, et al., *Appl. Catal., A* **306**, 108 (2006).
8. P. A. Chernavskii, A. S. Lermontov, G. V. Pankina, et al., *Kinet. Katal.* **43** (2), 292 (2002) [*Kinet. Catal.* **43** (2), 268 (2002)].